Effects of Active Fluxes in Gas Metal Arc Welding

Balázs Varbai[1,2*], Rita Kormos[1,3], Kornél Májlinger[1,4]

Abstract

In this paper the effects of active fluxes during gas metal arc welding (GMAW) were investigated. Eight different types of active fluxes, with different oxygen content, and $MnO - SiO_2$ flux mixtures were applied to the surface in 20 vol.% steps before welding. The used shielding gas was 82 % Ar + 18 % CO_2 (ISO 14175 M21) in all cases. Even small amount of active flux altered the weld face geometry, according to the cross sectional stereo micrographic images. The most significant effect on the internal form factor was experienced in case of MnO active flux, which decreased the internal form factor by 20 %. In case of the external form factor the applied SiO_2 active flux caused the biggest increase which is 37 %. In the hardness distribution and the microstructure of the joints, including the weld metal and the heath affected zone, no significant differences were experienced compared to the sample welded without any flux material.

Keywords

Gas metal arc welding, Active flux welding, Weld geometry, Structural steel, Microstructure

[1] Department of Materials Science and Engineering,
Budapest University of Techology and Economics
H-1111 Budapest, Bertalan Lajos str. 7., Hungary

[*] Corresponding author, e-mail: varbai@eik.bme.hu

1 Introduction

Nowadays the engineering industry has an increasing demand to enhance the welding technologies, in order to enable more productive and more efficient welding processes. One of the developing areas is joining thick plates with the minimum number of welding passes. Therefore deeper fusion depth is needed which increases the productivity areas, for example in case of welding high strength steels [1]). In order to increase productivity by reducing the welding passes, higher energy beam welding processes (e.g.: laser welding [2, 3], electron beam welding [4], plasma arc welding etc.) or novel welding methods (e.g.: friction stir welding [5]) can be used. In order to increase the productivity the usage of active fluxes gained attention in the recent times. By applying a thin layer of active flux on the surface prior welding, the penetration depth can be increased [6]. In case of tungsten inert gas (TIG) welding, with the usage of activated flux (A-TIG) 2-3 times deeper penetration can be achieved in Armco iron compared to the conventional TIG welding process [7]. In case of arc welding the driving force of the occurred flows in the weld pool can be originated from four different phenomena, the buoyancy, the surface-tension (which resulted in the so called Marangoni effect [7]), the high velocity movement of the arc plasma, and the Lorentz force [8, 9]. Regarding the physical background of these processes, different theoretical models were established [10, 11]. The models described; the vaporized ions from the flux play role in the increasing current density in the center of the welding arc, the applied flux reduces the surface tension and causes higher electric resistance, thus the size of the arc spot decreases [7]. All of the above-mentioned mechanisms have effect on the weld pool during A-TIG welding, however the main role is played by the reversed Marangoni flow [7-9]. The Marangoni effect is the mass transfer along an interface between two fluids due to surface tension gradient. In case of presence of active fluxes on the surface the mass transfer in the welding pool can be reversed from outward to inward which leads to reversed Marangoni flow. As a result of this inward convection the penetration depth is increasing [8, 9]. The same phenomena can be achieved by adding oxygen to the shielding gas [12]. Most of the researches [13-19]

of the application of active fluxes are based on TIG welding method. In case of gas-shielded metal arc welding (GMAW) the usage of active fluxes is not well published. During GMAW the effects of three types of active fluxes Fe_2O_3, SiO_2, $MgCO_3$ were investigated by Her-Yueh Huang [20] on AISI 1020 carbon steel plates with ER70S-6 welding wire and argon shielding gas. The researchers investigated the effects of active fluxes at three different 180 A, 200 A, 220 A welding current. In case of Fe_2O_3, SiO_2 and $MgCO_3$ fluxes the area of the weld metal and penetration depth increased for approximately ~50 %, and also the mechanical properties improved compared to the welds made without any flux material. In our research we investigated the effects of eight different active fluxes and mixtures in detail during GMAW using active shielding gas.

2 Materials and methods

The base material was 300x120x12 mm thick EN 1.0421 grade structural carbon steel, and was welded in as received (annealed) state. The chemical composition of the base material is 0.26 wt% C, 0.24 wt% Si, 0.42 wt% Mn, 0.06 wt% Cr, 0.01 wt% Ni, 0.04 wt% Al, 0.06 wt% Cu and Fe bal. The welding wire was G4Si1 (ER70S-6) material grade with Ø1 mm diameter. The chemical composition of the wire material is 0.10 wt% C, 1.00 wt% Si, 1.70 wt% Mn and Fe bal. Bead-on-plate run welds were made on the plates using Rehm Focus Puls 400 welding machine automated with Yamaha F1405-500 type linear drive in order to keep the welding parameters constant as shown in Table 1. The weld seams were made in a single pass with 100 mm lengths and with DC+ (direct current, wire positive) polarity. The oxide layer was removed with grinding from the surface, before the active fluxes were applied. As shielding gas ISO 14175 M21, 82 % Argon + 18 % CO_2 was applied.

Table 1 Fixed parameters applied during the welding tests

Fixed welding equipment parameters		
Wire feed	17.6	(m·min^{-1})
Welding speed	57	(cm·min^{-1})
Current	330	(A)
Arc voltage	40	(V)
Nozzle gap	15	(mm)
Shielding gas flow rate	12	(l·min^{-1})

The active flux material was applied on the plate surface before welding in a single, 0.12 mm thick layer. Eight grades of flux materials ($NaHCO_3$, $MgCO_3$, Fe_2O_3, Al_2O_3, TiO_2, CuO, MnO and SiO_2) were used in the first test series. After that mixtures of the two selected fluxes (MnO and SiO_2, because of their narrowing effect on the welding arc, therefore largest decreasing effects on the weld geometry form factors) were applied in 20 vol% steps. Therefore the specimen 40 % SiO_2

means a weld with an activating flux mixture of 60 vol% MnO and 40 vol% SiO_2. The corresponding quantities of the applied flux materials are given in Table 2. The fluxes were applied on the surface with a constant area, with same layer thickness. The differences of the quantities originated from the different densities of the flux materials. The oxygen contents of the active flux materials were calculated from the flux material quantities.

Table 2 Applied active flux types and their quantities for the welding tests

Active flux			
Composition	Quantity (g·cm^{-2})	Composition	Quantity (g·cm^{-2})
$NaHCO_3$	0.040	MnO	0.020
$MgCO_3$	0.015	20% SiO_2	0.024
Fe_2O_3	0.015	40% SiO_2	0.028
Al_2O_3	0.050	60% SiO_2	0.032
TiO_2	0.030	80% SiO_2	0.036
CuO	0.035	SiO_2	0.040

The weld morphology was investigated for macro- and microstructural characteristics. The face width and face height measurements were performed in minimum ten points using a calliper along the entire length of the weld seam. For microstructure investigations and hardness tests one metallographic specimen from approximately the middle of each weld line was made from the cross section of the weld seams. To measure the penetration depth on the etched metallographic specimens Olympus SZX16 type stereo microscope was used. The form factors of the weld geometry were determined on the stereo microscopic images. The external form factor is given as the ratio of the weld face width over the height and the internal form factor as the ratio of the face width over the penetration depth. The microstructure examinations were done using Olympus PMG3 type optical microscope, after the specimens were grinded up to 2500 grit sand paper and polished by 3 and 1 μm diamond suspension. Nital 2 % etchant (98 ml ethyl alcohol plus 2 ml nitric acid) was used to develop the microstructure. The Vickers hardness tests (HV10) were done on a KB Prüftechnik KB750 type universal hardness testing equipment. In order to determine the effects of the active fluxes the above mentioned measurements were made for all eight flux types and their mixtures according to Table 2. The results were compared to the weld made without flux material.

3 Results and discussion

During the welding process, spattering was experienced in case of SiO_2, CuO, TiO_2 and MnO fluxes. The biggest spattering was experienced during SiO_2 flux. This spattering resulted in the differences of the weld geometry measurements, most extensively in case of SiO_2 flux results. In the rest of the cases no unwanted increase in spattering was experienced.

3.1 Weld geometry

The cross sectional macrosection images of the weld metal can be found on Fig. 1. On these macrosections, also the penetration depth values were determined. Altogether, the results of the weld geometry measurements in case of pure fluxes are visible in Fig. 2, and in case of the flux mixtures in Fig. 3.
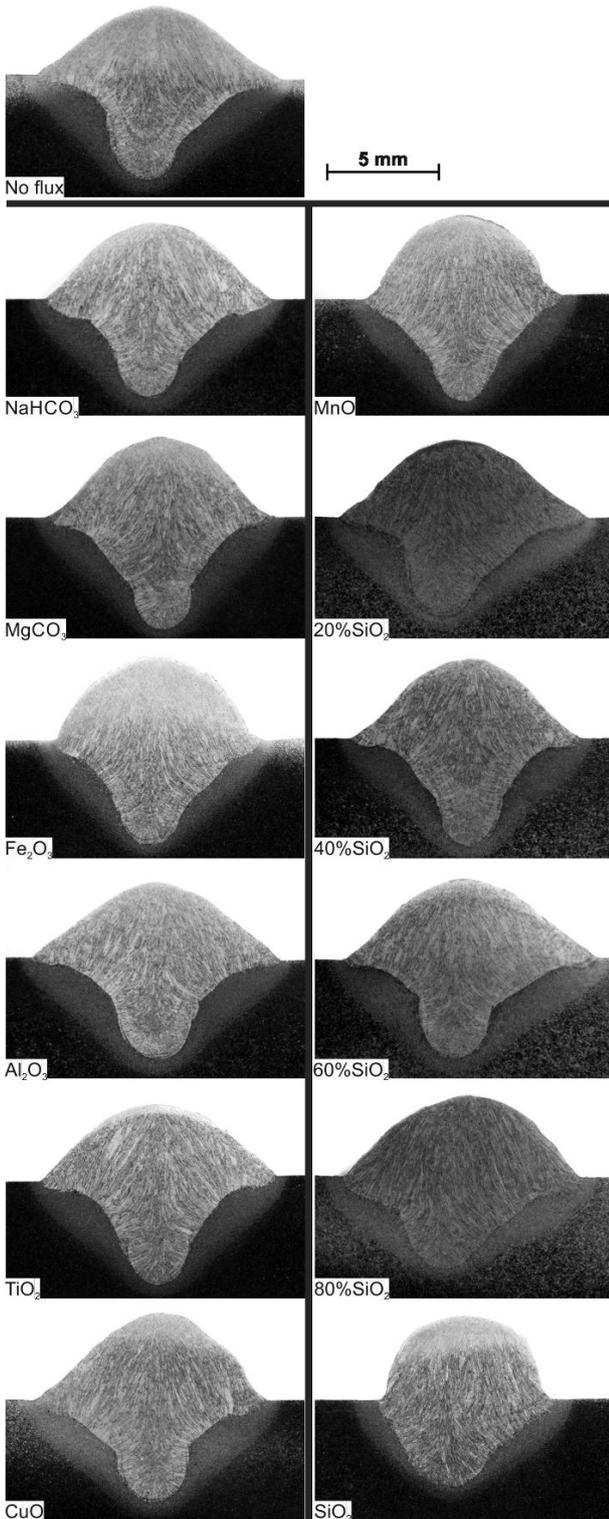
Fig. 1 Cross sectional stereo microscope micrograph of the welds welded with different active flux materials
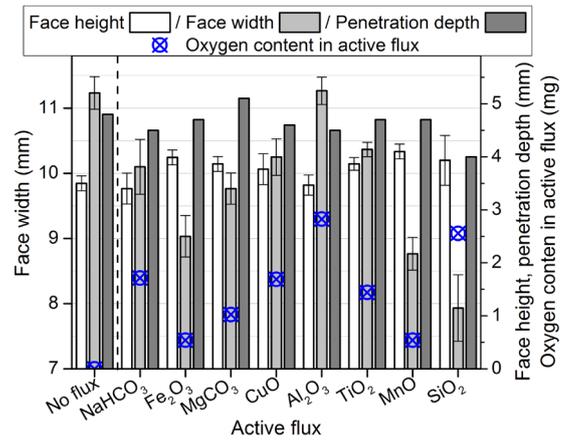
Fig. 2 Effects of the active fluxes on weld geometry and the oxygen content in the fluxes
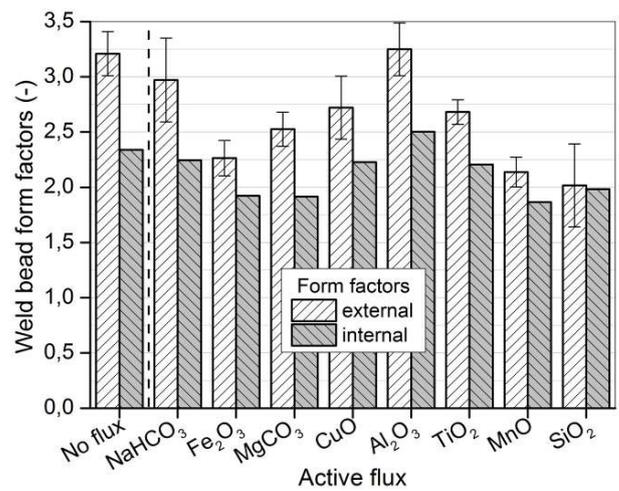
Fig. 3 Effects of active fluxes on the form factors of the welds

Compared to the welds made without any flux material the face width decreased in all cases except Al_2O_3. The average weld face width was the narrowest in case of SiO_2 (about 71 % of the weld with no flux). Using active fluxes the penetration depth values decreased slightly but increased by ~6 % in case of $MgCO_3$. The face height increased in all cases except when the welding was done with $NaHCO_3$ flux material. The biggest weld face height was achieved during welding with MnO flux. The oxygen content in the active flux shows direct proportion to the face width values and inverse proportion to the face height. Subsequently similar trends can be observed in the development of the external and internal form factors (Fig. 3). Compared to the no flux weld the external and internal form factors decreased in all cases except by the application of Al_2O_3. The largest effect was measured in case of MnO and SiO_2 fluxes (~33-37 % less external and 21-15 % less internal form factor of the weld) therefore the mixture of these two active fluxes was investigated more detailed.

During the investigation of the effects of SiO_2 – MnO active flux mixtures (Fig. 4), the maximum face width was achieved with the mixture of 60 % SiO_2 and 40 % MnO, while all of the mixtures gave wider welds compared to the pure SiO_2 and MnO fluxes. Compared to the weld with no flux the values were smaller (except the 60 % SiO_2 mixture) indicating the fluxes lowered the surface tension and the melt's viscosity. The deepest weld penetration was measured in case of 40 % SiO_2, which is slightly deeper than in case of no flux weld, in the other cases smaller penetration was detected. The weld face height has not changed significantly on the effect of mixing the two fluxes to each other and it was about 13 % higher than in case of no flux. The oxygen content in the active flux mixtures shows no correlation to the weld geometry as extensive spattering was experienced in case of welding with SiO_2 fluxes. The external and internal form factors (Fig. 5) followed the trends of the weld width changes. Both the external and internal form factors were smaller compared to the no flux weld (9 % and 1 % smaller respectively).
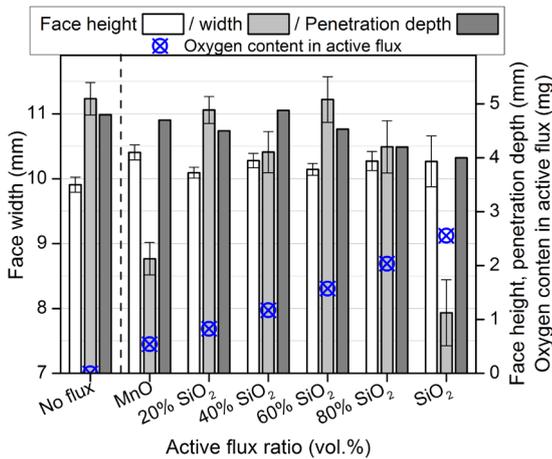
Fig. 4 Effects of active flux mixtures on weld geometry and oxygen content in active fluxes
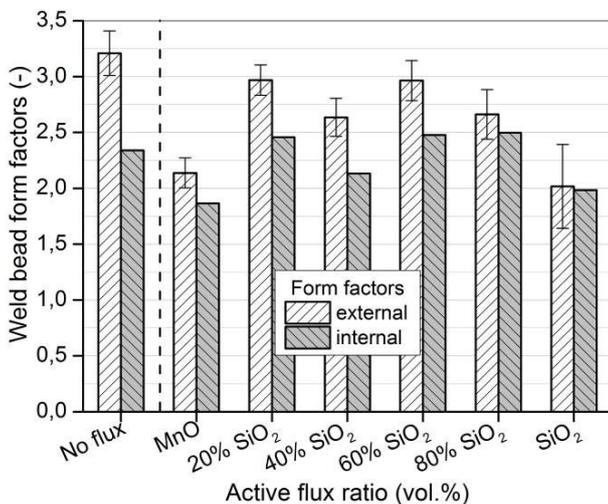
Fig. 5 Effects of active flux mixtures on weld form factors

In case of the SiO_2 and MnO flux mixtures both the external and internal form factors increased compared to the pure fluxes. 20% SiO_2 + 80% MnO and 60% SiO_2 + 40% MnO mixtures showed the biggest increase in the external form factor. In case of the internal form factor the 20%, 60% and 80% SiO_2 mixtures showed roughly the same increase, which is 32-34%.

The overall weld geometry showed increasing width of the weld root (Fig. 1).

3.2 Microstructure investigations

The microstructure investigations were made for all samples. The microstructure of the base material, the weld metal and the heat affected zone (HAZ) are shown in Fig. 6. in cases when the used active flux material had the most significant effect on the weld geometry ($MgCO_3$, MnO, 40 % SiO_2 + 60 % MnO and SiO_2). The weld metal and the HAZ had a coarse grain size and needle like ferrite and perlite grains in all cases. From Fig. 6 it is visible, the fluxes had basically no effect on the grain size or the microstructure of the investigated areas, only the macroscopic appearance (for weld geometry see Fig. 1) was altered.

3.3 Hardness measurements

The Vickers hardness measurements were done on the metallographic specimens in the weld metal, HAZ and base metal, in minimum 5 points. The hardness of the base metal was measured 133±4 HV10. The results of the hardness measurements are listed in Table 3. No significant difference can be seen in the results of the hardness measurements neither in the weld material nor in the HAZ for the different samples. The used active fluxes and mixtures had no significant effect on the HV10 hardness values, all samples were in the scattering range.

Table 3 Effects of active fluxes on the hardness values of the welded joints

Active flux type	Hardness (HV10)		Active flux type	Hardness (HV10)	
	Weld	HAZ		Weld	HAZ
No flux	206±5	165±2			
NaHCO$_3$	210±2	172±3	MnO	214±3	170±4
Fe$_2$O$_3$	210±5	171±4	20% SiO$_2$	209±3	173±3
MgCO$_3$	209±5	174±3	40% SiO$_2$	207±2	176±1
CuO	204±4	171±2	60% SiO$_2$	204±6	170±5
Al$_2$O$_3$	208±3	172±5	80% SiO$_2$	210±5	167±5
TiO$_2$	210±3	169±4	SiO$_2$	211±4	175±3
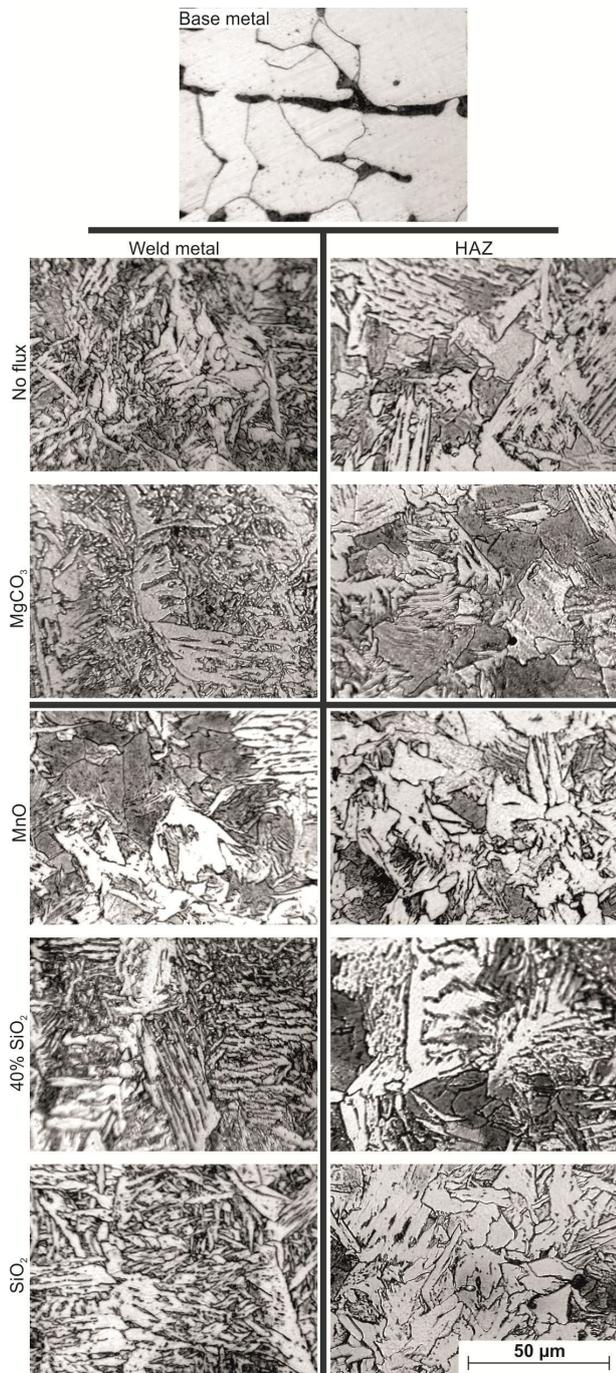
Fig. 6 Effects of active fluxes on weld metal and HAZ microstructure

4 Conclusion

From the above mentioned investigations the following conclusions can be drawn. In case of GMAW of low carbon steels using active shielding gas (82 % Argon+18 % CO_2) small amounts of active fluxes can alter the geometry and also the form factors of the welds compared to the normal GMAW welded sample without any active flux material:

- The biggest increase in the internal form factor can be achieved with Al_2O_3 active flux, which is about 7%.
- The oxygen content in the active flux shows direct proportion to the face width values and inverse proportion to the face height.

- In case of the SiO_2-MnO flux mixtures large fluctuations in the internal and external form factors (27% and 30%) was observed.
- The biggest and lowest external form factor was observed in case of 20% SiO_2 and 40% SiO_2 mixtures respectively.
- The biggest and lowest internal form factor was observed in case of 80% SiO_2 and 40% SiO_2 mixtures respectively.
- The changes in weld geometry do not affect the microstructure or the hardness of the joints, both in the weld and in the HAZ, the microstructural characteristics and the hardness values were basically the same.

In case of low carbon steel welding active fluxes had influence the GMAW process, but not as much as it was reported in case of stainless steel welded by TIG welding process.

References

[1] Gáspár, M., Balogh, A. "GMAW experiments for advanced (Q+T) high strength steels." *Production Processes and Systems*. 6(1), pp. 9-24. 2013.

[2] Dobránszky, J., Lőrinc, Zs., Gyímesi, F., Szigethy, A., Bitay, E. "Laser welding of lean duplex stainless steels and their dissimilar joints." In: *8th European Stainless Steel and Duplex Stainless Steel Conference*, Graz, Austria, April 28-30, 2015, pp. 138-147.

[3] Kálazi, Z., Meiszterics, Z., Janó, V., Szabados, O., Magyar, Zs., Buza, G. "Laser welding of steel plates with divided beam." *Materials Science Forum*. 659, pp. 483-488. 2010.
https://doi.org/10.4028/www.scientific.net/MSF.659.483

[4] Węglowski, M. St., Błacha, S., Phillips, A. "Electron beam welding – Techniques and trends – Review." *Vacuum*. 130, pp. 72-92. 2016.
https://doi.org/10.1016/j.vacuum.2016.05.004

[5] Meilinger, Á., Török, I. "The importance of friction stir welding tool." *Production Processes and Systems*. 6, pp. 25-34. 2013.

[6] Dobránszky, J., Sándor, T. "Increasing the productivity of tungsten inert gas welding." *Bid-Isim Welding and Material Testing*. 24, pp. 8-11. 2015.

[7] Sándor, T., Mekler, C., Dobránszky, J., Kaptay, G. "An improved theoretical model for A-TIG welding based on surface phase transition and reversed Marangoni flow." *Metallurgical and Materials Transactions A-Physical Metallurgy and Materials Science*. 44A, pp. 351-361. 2013.
https://doi.org/10.1007/s11661-012-1367-2

[8] Lu, S., Fujii, H., Sugiyama, H., Tanaka, M., Nogi, K. "Weld Penetration and Marangoni Convection with Oxide Fluxes in GTA Welding." *Materials Transactions*. 43(11), pp. 2926-2931. 2002.
https://doi.org/10.2320/matertrans.43.2926

[9] Kou S. "*Welding Metallurgy*." Chapter 4, pp. 97-117. John Wiley & Sons, Inc., Hoboken, New Jersey. 2003.

[10] Sándor, T., Dobránszky, J. "Comparison of penetration profiles of different TIG process." In: *Stainless Steel World Conference*, Maastricht, Netherlands, Nov. 10-12, 2009, pp. 1-16.

[11] Sándor, T., Dobránszky, J. "The experiences of activated tungsten inert gas (ATIG) welding applied on 1.4301 type stainless steel plates." *Materials Science Forum*. 537-538, pp. 63-70. 2007. https://doi.org/10.4028/www.scientific.net/MSF.537-538.63

[12] Hidetoshi, F., Sato, T., Lu, S., Nogi, K. "Development of an advanced A-TIG (AA-TIG) welding method by control of Marangoni convection." *Materials Science and Engineering: A*. 495, pp. 296-303. 2008. https://doi.org/10.1016/j.msea.2007.10.116

[13] Chern, T.-S., Tseng, K.-H., Tsai, H.-L. "Study of the characteristics of duplex stainless steel activated tungsten inert gas welds." *Materials and Design*. 32, pp. 255-263. 2011. https://doi.org/10.1016/j.matdes.2010.05.056

[14] Vidyarthy, R. S., Dwivedi, D. K. "Activating flux tungsten inert gas welding for enhanced weld penetration." *Journal of Manufacturing Processes*. 22, pp. 211-228. 2016. https://doi.org/10.1016/j.jmapro.2016.03.012

[15] Cai, Y., Luo, Z., Huang, Z., Zeng, Y. "Effect of cerium oxide flux on active flux TIG welding of 800 MPa super steel." *Journal of Materials Processing Technology*. 230, pp. 80-87. 2016. https://doi.org/10.1016/j.jmatprotec.2015.11.008

[16] Ramkumar K.D., Varma, J. L. N., Chaitanya, G., Choudhary, A., Arivazhagan, N., Narayanan, S. "Effect of autogeneous GTA welding with and without flux addition on the microstructure and mechanical properties of AISI 904L joints." *Materials Science and Engineering: A*. 636, pp. 1-9. 2015. https://doi.org/10.1016/j.msea.2015.03.072

[17] Dhandha, K. H., Badheka, V. J. "Effect of activating fluxes on weld bead morphology of P91 steel bead-on-plate welds by flux assisted tungsten inert gas welding process." *Journal of Manufacturing Processes*. 17, pp. 48-57. 2015. https://doi.org/10.1016/j.jmapro.2014.10.004

[18] Tseng, K.-H., Chuang, K.-J. "Application of iron-based powders in tungsten inert gas welding for 17Cr–10Ni–2Mo alloys." *Powder Technology*. 228, pp. 36-46. 2012. https://doi.org/10.1016/j.powtec.2012.04.047

[19] Klobčar, D., Tušek, J., Bizjak, M., Simončič, S., Lešer, V. "Active flux tungsten inert gas welding of austenitic stainless steel AISI 304." *METABK*. 55(4), pp. 617-620. 2016.

[20] Huang, H.-Y. "Effects of activating flux on the welded joint characteristics in gas metal arc welding." *Materials and Design*. 31, pp. 2488-2495. 2010. https://doi.org/10.1016/j.matdes.2009.11.043